Eur. Phys. J. A **12**, 405–411 (2001)

THE EUROPEAN PHYSICAL JOURNAL A

Modified Glauber model for the total reaction cross-section of $^{12}C + ^{12}C$ collisions

M.Y.H. Farag[a]

Physics Department, Faculty of Science, Cairo University, Cairo, Egypt

Received: 26 January 2001 / Revised version: 30 July 2001
Communicated by P. Schuck

Abstract. Glauber's theory has been adopted to calculate the total heavy-ion reaction cross-sections at high energies. At relatively low energies, Glauber's total reaction cross-section has been modified in order to take into account the Coulomb field effect and is called modified Glauber model I. In addition to the Coulomb field effect, the nuclear effect has also been taken into account in the Glauber model and is called modified Glauber model II. An analytical expression for the transparency function for heavy-ion reactions, involving the nuclear densities of the colliding ions and the nucleon-nucleon cross- section, has been obtained within the framework of the modified Glauber models I and II. The transparency and the total reaction cross-sections of the $^{12}C + ^{12}C$ collisions are calculated at different bombarding energies. The obtained results are in good agreement with the experimental data and with previous theoretical calculations.

PACS. 24.10.Ht Optical and diffraction models – 24.10.Lx Monte Carlo simulations (including hadron and parton cascades and string breaking models) – 24.60.Dr Statistical compound-nucleus reactions – 25.70.Gh Compound nucleus

1 Introduction

The total reaction cross-sections for heavy-ions have been studied extensively, both theoretically and experimentally [1–10] for a long time. The total reaction cross-section is one of the most fundamental quantities characterizing the nuclear reactions [9–12]. At high energies, the Glauber model [13] has successfully described the heavy-ion reaction cross-section based on the independent individual nucleon-nucleon collisions in the overlap zone of the colliding nuclei. This model has been extended to low energies by taking into account the effect of the Coulomb field which let the straight-line trajectory of the colliding nuclei to be deviated [14–22]. This approach is called the Coulomb-modified Glauber model or the modified Glauber model I. Then, this model has been refined [21–23] to take into account the nuclear-potential effect on the trajectory. This formalism is referred to as the modified Glauber model II and has been applied satisfactorily to the elastic-scattering reaction $^{16}O + ^{12}C$ and $^{16}O + ^{28}Si$ at $E_{Lab} = 1503$ MeV [22].

In the present work, the elastic scattering of $^{12}C + ^{12}C$ at different energies is studied using both the modified Glauber models I and II. Section 2 deals with the formalisms of both models. The calculations and results are given in sect. 3. Discussion and conclusions are presented in sect. 4.

2 Theory

The standard Glauber form for the reaction cross-section at high energies, where the Coulomb effect plays no significant role is expressed [8,17,19,24–27] as:

$$\sigma_R = 2\pi \int_0^\infty b\mathrm{d}b[1 - T(b)]\,, \tag{1}$$

where $T(b)$, the transparency function, is the probability that at an impact parameter b the projectile pass through the target without interacting. This function $T(b)$ is calculated in the overlap region between the projectile and target where the interactions are assumed to result from single nucleon-nucleon collision and is given by

$$T(b) = \exp(-\sigma_{NN}\varkappa(b))\,, \tag{2}$$

where σ_{NN} is the nucleon-nucleon total cross-section and $\varkappa(b)$ is the overlap integral of the nuclear densities along a straight line characterized by the impact parameter b. For light nuclei with $A \leq 40$ [24], the density distribution is assumed to be Gaussian [14–17,23,24,26]:

$$\rho_i(r) = \rho_i(0)\exp(-r^2/a^2)\,; \qquad (i = \mathrm{P}, \mathrm{T}) \tag{3}$$

[a] e-mail: myhfarag@hotmail.com

where a_i and $\rho(0)$ are the diffuseness and the central nuclear density, respectively; both are treated as free adjustable parameters to reproduce the experimental nuclear surface, since most of the reaction cross-section comes from the surface region:

$$\rho_i(0) = \frac{A}{(a_i\sqrt{\pi})^3} \tag{4}$$

and the diffuseness, a, is related to the root-mean-square radius $\langle r^2\rangle^{1/2}$ [17,24] by

$$a = 0.8165\langle r^2\rangle^{1/2}\,. \tag{5}$$

The nuclear density (eq. (3)) is considered for both projectile and target. Therefore, the integral, given in eq. (5), can be evaluated analytically, giving the expression

$$T(b) = \exp\left[-\varkappa_0 \exp\left(-\frac{b^2}{a_{\rm P}^2 + a_{\rm T}^2}\right)\right]\,, \tag{6}$$

where $\varkappa_0$ is given by

$$\varkappa_0 = \frac{\pi^2\sigma_{\rm NN}\rho_{\rm P}(0)\rho_{\rm T}(0)a_{\rm P}^3 a_{\rm T}^3}{a_{\rm P}^2 + a_{\rm T}^2}\,. \tag{7}$$

The nucleon-nucleon total cross-section $\sigma_{\rm NN}$ is averaged over the experimental proton-proton and proton-neutron total cross-section through the relation [17,23,26,28,29]

$$\sigma_{\rm NN} = \frac{(Z_{\rm P}Z_{\rm T} + N_{\rm P}N_{\rm T})\sigma_{\rm pp} + (Z_{\rm P}N_{\rm T} + Z_{\rm T}N_{\rm P})\sigma_{\rm pn}}{A_{\rm P}A_{\rm T}}\,, \tag{8}$$

which has the proton-proton cross-section $\sigma_{\rm pp}$, equal to the neutron-neutron cross-section $\sigma_{\rm nn}$ and where $A_{\rm P}, A_{\rm T}, Z_{\rm P}, Z_{\rm T}$ and $N_{\rm P}, N_{\rm T}$ are mass, charge and neutron numbers for the projectile and the target, respectively.

The Glauber model agrees very well with the experimental data at high energies. However, this model fails to reasonably describe the collisions induced at relatively low energies. This disagreement is due to the significant role played by the Coulomb repulsive potential whose effects are obvious in the low-energy range. Such a Coulomb effect breaks the characteristic Glauber assumption that the projectile travels along straight-line trajectories.

Several attempts have been made to include the Coulomb effect into the Glauber formalism [2,14,15,18, 19,28]. The most successful approach, based on the WKB approximation for the phase shifts, replaces the impact parameter b in the transparency function $T(b)$ in eq. (1) by the distance b' of the closest approach of the deviated projectile trajectory due to the Coulomb effect. Therefore, by substituting the transparency function $T(b')$ for $T(b)$ in eq. (1) with $b'(b)$, being the classical distance of the closest approach, thus the reaction cross-section can be expressed [8,19,21,26] as

$$\sigma_{\rm R}^{\rm C} = 2\pi\int_0^\infty b{\rm d}b(1 - T(b'))\,. \tag{9}$$

The parameter b' corresponds to the distance of the closest approach along the Coulomb trajectory, and is related to the impact parameter b according to [14–16,20,21,23,26]:

$$b' = \frac{1}{k}\left(\eta + \sqrt{\eta^2 + k^2b^2}\right)\,, \tag{10}$$

which is the solution of the equation

$$1 - \frac{2\eta}{kb} - \frac{L^2}{k^2b^2} - \frac{V_{\rm n}(b)}{E} = 0.0\,, \tag{11}$$

where E is the kinetic energy in the centre-of-mass system, L is the angular momentum, $V_{\rm n}(b)$ is the real part of the optical potential, k is the projectile wave number and η is the Sommerfeld parameter defined [14,15,19,23,26] as

$$\eta = \frac{Z_{\rm P}Z_{\rm T}e^2}{\bar{h}v}\,. \tag{12}$$

When the real part of the optical potential $V_{\rm n}(b)$ is taken to be zero, eq. (10), which is a solution of eq. (11) can be rewritten as

$$b^2 = \left(1 - \frac{V_{\rm C}(b')}{E_{\rm cm}}\right)b'^2\,, \tag{13}$$

where $V_{\rm C}(b')$ is the Coulomb potential at a distance b' from the center of the target and is defined as

$$V_{\rm C}(b') = \frac{1.44Z_{\rm P}Z_{\rm T}}{b'} = \frac{\eta\bar{h}v}{b'}\,. \tag{14}$$

If we replace $V_{\rm C}(b')$ by its value $V_{\rm C}$ at the strong absorption radius, then, eq. (13) becomes

$$b^2 = \left(1 - \frac{V_{\rm C}}{E_{\rm cm}}\right)b'^2\,. \tag{15}$$

The strong absorption radius $R_{\rm sab}$ is defined as the distance for which the transparency function $T(b) = \frac{1}{2}$, *i.e.* the distance where the incident particle has the same probability to be absorbed as to be reflected. The strong absorption radius $R_{\rm sab}$ is given by [26]:

$$R_{\rm sab}^2 = (a_{\rm P}^2 + a_{\rm T}^2)\,(\ln\varkappa_0 + 0.3665)\,. \tag{16}$$

Taking into consideration eq. (15), then eq. (9) becomes

$$\sigma_{\rm R}^{\rm C} = 2\pi\left(1 - \frac{V_{\rm C}}{E_{\rm cm}}\right)\int_0^\infty b'{\rm d}b'(1 - T(b'))\,. \tag{17}$$

From this equation and eq. (1), we find that

$$\sigma_{\rm R}^{\rm C} = \left(1 - \frac{V_{\rm C}}{E_{\rm cm}}\right)\sigma_{\rm R}\,. \tag{18}$$

Using a similar procedure, eq. (11) can be solved taking into consideration the effect of the real part of the optical potential $V_{\rm n}(b)$. So, at the strong absorption radius, the distance of the closest approach in the presence

Table 1.

E/A (MeV)	25	30	38	40	49	85	94	120	200	342.5
σ_{NN} (fm^2)	24.1	19.6	14.6	13.5	10.4	6.1	5.5	4.5	3.2	2.84
α_{NN}	0.85	0.87	0.89	0.9	0.94	1	1.07	0.7	0.6	0.26

of the nuclear and Coulomb fields is given by the following expression:

$$r_{CN}^2 = b^2 / \left(1 - \frac{V_C}{E_{cm}} - \frac{V_n}{E_{cm}}\right). \quad (19)$$

Therefore,

$$\sigma_R^{CN} = 2\pi \left(1 - \frac{V_C}{E_{cm}} - \frac{V_n}{E_{cm}}\right) \int_0^\infty r_{CN} dr_{CN} (1 - T(r_{CN})). \quad (20)$$

Then,

$$\sigma_R^{CN} = \left(1 - \frac{V_C}{E_{cm}} - \frac{V_n}{E_{cm}}\right) \sigma_R. \quad (21)$$

It is clear that eqs. (18) and (21) represent the total reaction cross-sections for the modified Glauber models I and II, respectively. The potential V_n is taken in the Woods-Saxon form as [23]:

$$V_n = -V_0 \Big/ \left(1 + \exp\left(\frac{R_{sab} - r_V(A_P^{1/3} + A_T^{1/3})}{a_V}\right)\right). \quad (22)$$

3 Calculation and results

In the present work, the elastic scattering of $^{12}C + ^{12}C$ at different bombarding energies ranged from E_{Lab} = 25 MeV/nucleon to 342.5 MeV/nucleon is studied. The calculations are done for the original Glauber model (eq. (1)), the modified Glauber model I (eq. (18)) and the modified Glauber model II (eq. (21)). The calculations of the total reaction cross section imply the calculation of the transparency function $T(b)$ deduced from eq. (2). The Gaussian density distributions are considered (eq. (3)) for both projectile and target with the parameters $\rho_0(0) = 0.2974$ fm^{-3} and $a = 1.935$ fm [17].

The averaged nucleon-nucleon cross-sections σ_{NN} are given in table 1 [15,17].

The transparency function $T(b)$ is calculated for different energies. The results of the calculations at energies 300, 1020 and 2400 MeV are plotted in fig. 1 as a function of the impact parameter b. This figure shows that for the relatively high energies (200 MeV/A), $T(b)$ tends to zero faster than for the relatively lower energies (25 MeV/A). However, a saturation value unity for impact parameter around 8 fm has been observed for all cases. The effect

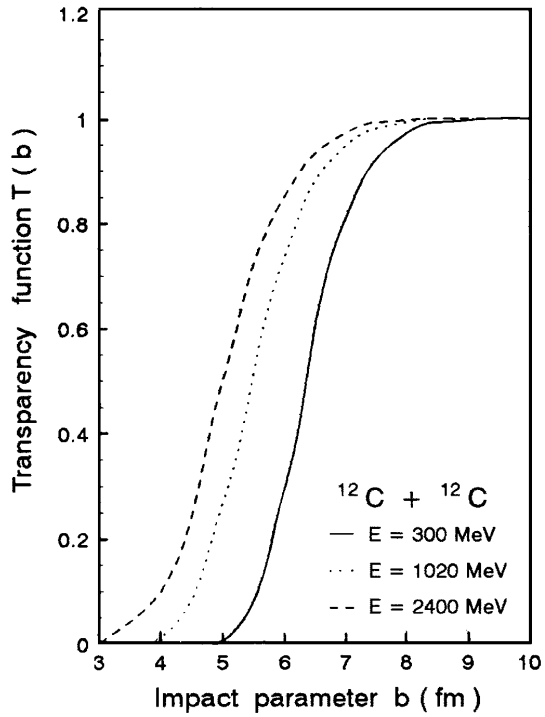

Fig. 1. The transparency function $T(b)$ as a function of the impact parameter for different bombarding energies ranged from 25 MeV/nucleon up to 200 MeV/nucleon of $^{12}C + ^{12}C$ collisions.

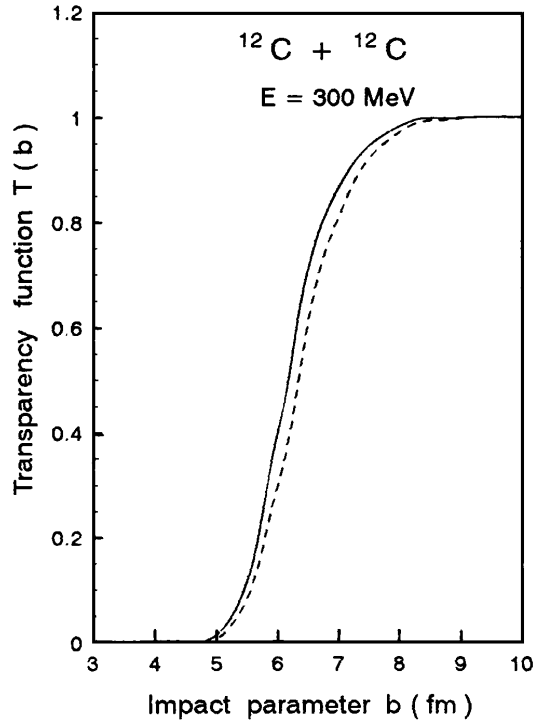

Fig. 2. The transparency function $T(b)$ for the original Glauber model is given by the dashed curve, while the solid curve represents the transparency function for the modified Glauber model I for the energy 25 MeV/nucleon.

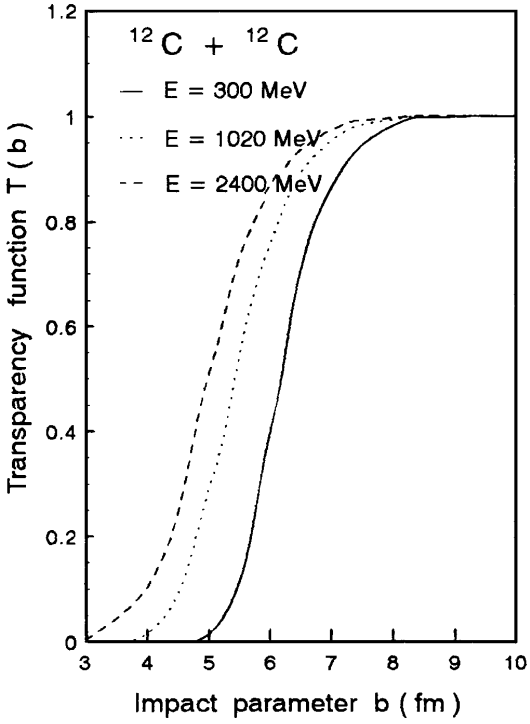

Fig. 3. The transparency function of the modified Glauber model I for different bombarding energies ranged from 25 MeV/nucleon up to 200 MeV/nucleon.

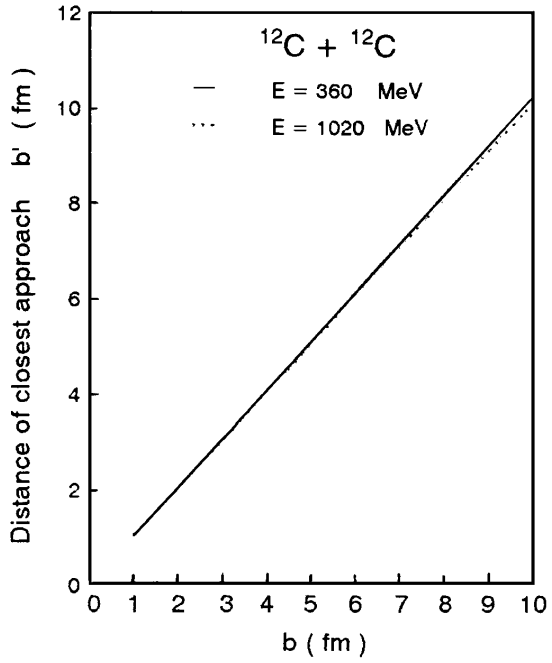

Fig. 4. The distance b' of the closest approach as a function of the impact parameter b for energies: $E = 30$ MeV/nucleon (solid line) and 85 MeV/nucleon (dotted line).

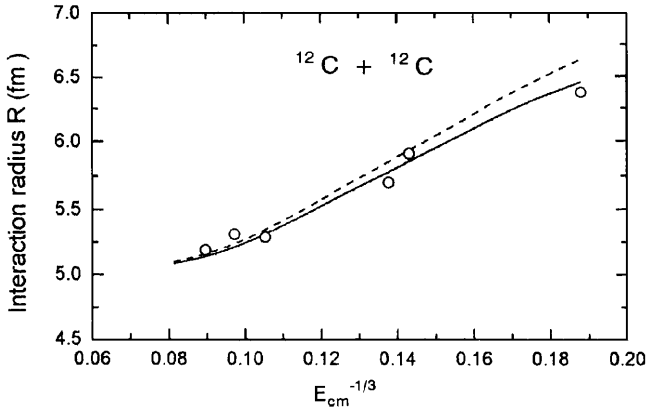

Fig. 5. The interaction radius R as a function of bombarding energies, $E_{\rm cm}^{-1/3}$, for the ^{12}C + ^{12}C collisions; the dashed curve is for the case of the original Glauber model, while the solid curve is for the modified Glauber model I and the open circle is for the experimental values [30].

of the Coulomb field for the bombarding energy 300 MeV (25 MeV/A) is shown in fig. 2. The effect of the Coulomb field on the transparency function is to reduce it to zero faster for low impact parameter. Similar results are shown in fig. 3 for different bombarding energies. The distance of the closest approach is drawn *versus* the impact parameter b for different bombarding energies as shown in fig. 4. From this figure, it is clear that the distance of the closest approach is inversely proportional to the energy.

The interaction radius R is related to the reaction cross-section by the formula [30]

$$R = \frac{\eta}{k}\left[1 + \left(1 + \frac{k^2}{\eta^2}\frac{\sigma_{\rm R}}{10\pi}\right)^{\frac{1}{2}}\right], \qquad (23)$$

where

$$\frac{\eta}{k} = 0.72 Z_{\rm P} Z_{\rm T} \, / E_{\rm cm}\,. \qquad (24)$$

By substituting the calculated reaction cross-section $\sigma_{\rm R}$ and the modified reaction cross-section due to the Coulomb field $\sigma_{\rm R}^{\rm C}$ into eq. (23), various values for the interaction radius R can be extracted. The relation between R and $E_{\rm cm}^{-1/3}$ for the ^{12}C + ^{12}C collision is shown in fig. 5. One notes that the dependence of R on the energy is weak ($R \propto E_{\rm cm}^{-1/3}$) at low energies and becomes stronger at intermediate energies. One sees that the nucleus-nucleus reaction cross-section is controlled by the mean field at low energies and by nucleon-nucleon interaction at intermediate energies.

The total reaction cross-sections are calculated taking into consideration the effects of the modified Glauber models I and II. The obtained results for the calculations of the reaction cross-section without modification and with the modified Glauber I are shown in fig. 6. The resultant $\sigma_{\rm R}$ decreases systematically. This indicates that $\sigma_{\rm R}$ is sensitive to $\sigma_{\rm NN}$. The obtained results are in good agreement with the experimental data [10] and with the other theoretical calculations [29]. The modifications improve the resulting total reaction cross-section. The effect of the modified Glauber model II is shown by calculating the real part of the optical potential (eq. (22)). In this work, the calculations are done for $E_{\rm Lab} = 360$ and 1020 MeV. The parameters of eq. (22) for the energies 360

Table 2.

E (MeV)	V_0 (MeV)	r_V (fm)	a_V (fm)	σ_R (mb)	σ_R^C (mb)	σ_R^{CN} (mb)	σ_R^{exp} (mb)
360	120	0.79	0.7	1261.94	1203.4	1223.52	1315 ± 40
1020	120	0.71	0.84	987.34	968.95	984.55	984.55

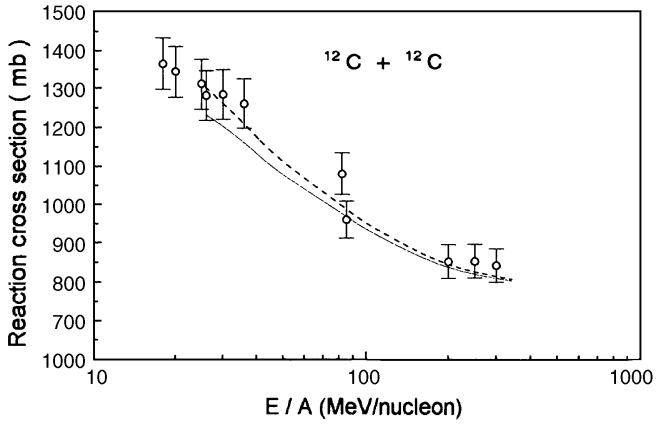

Fig. 6. The energy dependence of the total reaction cross-section for the $^{12}C + ^{12}C$ collisions. The dashed curve is for the original Glauber model while the solid curve is for the modified Glauber Model I. The experimental values are shown as open circle [30].

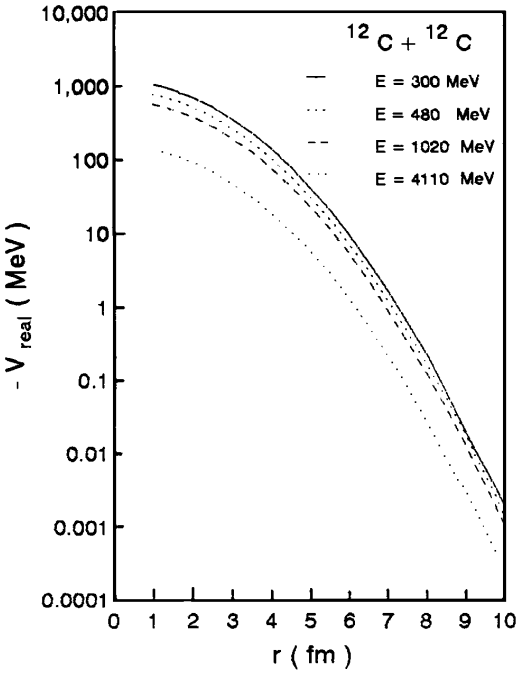

Fig. 7. The real part of the optical potential obtained in the modified Glauber model I for different bombarding energies.

and 1020 MeV are given in table 2. The resulting values for the total reaction cross-section σ_R, modified total reaction cross-section due to the effect of the Coulomb trajectory σ_R^C and the modifications due to both the Coulomb and nuclear effects σ_R^{CN} are also given in table 2. The experimental nucleus-nucleus σ_R^{exp} are given in the last column of table 2. It is clear from the results given in table 2, that the total reaction cross-section σ_R^{CN} for the modified Glauber II is very close to the experimental values especially for $E = 85$ MeV/nucleon. This means that the modified Glauber II improves the resultant reaction cross-sections.

Within the Glauber model [13], one can obtain, from the phase shifts, the nucleus-nucleus optical potential $V(r)$ for the values of the distance of closest approach for which $b' \geqslant b$ according to the integral transform [14,15]:

$$V(r) = \frac{2\bar{h}V}{\pi r}\frac{\mathrm{d}}{\mathrm{d}r}\int_r^\infty \frac{\delta(b')}{(b'^2 - r^2)^{\frac{1}{2}}} b'\mathrm{d}b' \,, \qquad (25)$$

where

$$\delta\ (b') = \frac{1}{2}\ \sigma_{NN}\ (\alpha_{NN}\ + i)\varkappa\ (b') \,, \qquad (26)$$

where α_{NN} is the ratio of the real to the imaginary part of the forward nucleon-nucleon scattering amplitude. In the optical limit, this ratio is also the ratio of the real to the imaginary part for the nucleus-nucleus complex phase shift and the same for the optical potential [17]. It expresses the relative importance of the refraction compared to the absorption in the nucleus-nucleus amplitude. The values σ_{NN} and α_{NN}, associated with microscopic nucleon-nucleon scattering, have been obtained by interpolating the experimental values at the corresponding energies. These parameters are given in table 1. The value of $\varkappa(b')$, defined in eq. (26), is given by

$$\varkappa\ (b') = \varkappa_0 \exp\left(-\frac{b'^2}{a_P^2 + a_T^2}\right) \,, \qquad (27)$$

where $\varkappa_0$ is given by

$$\varkappa_0 = \frac{\pi^2 \rho_P(0)\rho_T(0) a_P^3 a_T^3}{a_P^2 + a_T^2} \,. \qquad (28)$$

Therefore, the real part of the optical potential obtained is:

$$V_{real}(r) = -\frac{\pi^{3/2}\hbar v \rho_P(0)\rho_T(0) a_P^3 a_T^3 \sigma_{NN}\alpha_{NN}}{2(a_P^2 + a_T^2)^{3/2}} \times \exp\left(-\frac{r^2}{a_P^2 + a_T^2}\right) \,. \qquad (29)$$

The calculations of eq. (29) at different bombarding energies from 300 to 4110 MeV, are shown in fig. 7. This figure shows that the results for the real potential for the modified Glauber I, are deeper for low energies than for higher ones.

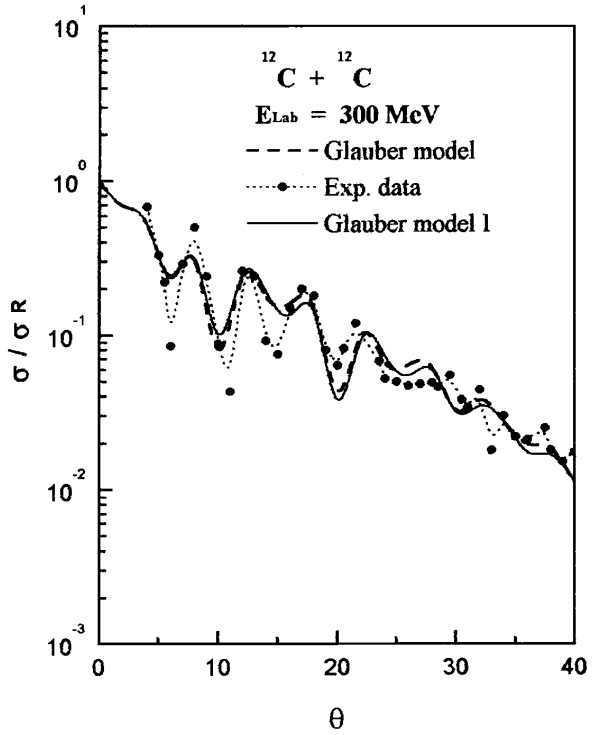

Fig. 8. The theoretical elastic-scattering differential cross-section for ^{12}C + ^{12}C system at $E_{\rm Lab} = 300$ MeV. The dashed curve is for the standard Glauber model, while the solid curve is for the modified Glauber model I. The experimental data [31] are shown as solid circles.

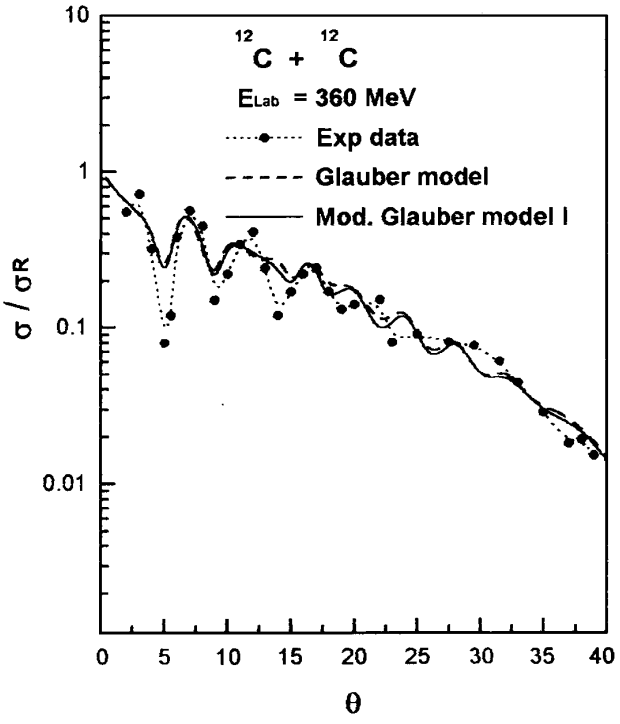

Fig. 9. Elastic angular distributions for the scattering of the ^{12}C + ^{12}C collisions at $E_{\rm Lab} = 360$ MeV. The dashed curve is for the standard Glauber model while the solid curve is for the modified Glauber model I. The experimental values [7] are shown as a dotted curve.

The calculated elastic-scattering differential cross-sections for the ^{12}C + ^{12}C at energies 300 and 360 MeV are shown in figs. 8 and 9, respectively. The obtained results are show a reasonable agreement with the experimental data [7,31]. Therefore, one can conclude that the modified Glauber models provide a suitable description of the data for the elastic scattering of the ^{12}C + ^{12}C collisions at $E_{\rm Lab} = 300$ and 3660 MeV.

4 Discussion and conclusions

In the present work, analytical expressions for the heavy-ion reaction cross-section within the framework of the Glauber model are presented. The reaction considered here, is the ^{12}C + ^{12}C collisions at bombarding energies ranging from 25 up to 342.5 MeV/nucleon. The density of this nucleus is considered to be of Gaussian form. The description of the trajectory is modified by taking into consideration the effect of the Coulomb field, *i.e.*, the modified Glauber I. The nuclear field in addition to the Coulomb filed is also taken into consideration, *i.e.*, the modified Glauber II. Both modifications improve the description of the total reaction cross-section. This has been done by evaluating the transparency of the target towards the projectile at the distance of the closest approach of the deviated projectile trajectory.

It is well known that the nucleus-nucleus elastic scattering is essentially determined by a small range of impact parameters, corresponding to the surface collisions. Nuclear transparency is an effect associated with the nuclear surface, which is diffuse. The lower partial waves are totally absorbed as illustrated by the transparency function $T(b)$. In the surface region, the nuclear potential and also the Coulomb potential (about 8 MeV) are small compared to the kinetic energy. Therefore, the straight-line trajectory assumption is certainly a reasonable approximation. For smaller energies $E/A = 25$ and 30 MeV, the optical model analysis shows that the absorption is so strong for values of b less than 5 fm that the partial waves in the region of the nuclear rainbow can hardly contribute to the cross-section. The situation is rather different for energies greater than $E/A = 85$ MeV where the total absorption takes place at smaller impact parameter. At $E/A = 85$ MeV and greater, the nuclei densities have more overlap and then higher-order effects, such as nucleon correlation, probably become important. For energy range $E/A = 100$–200 MeV, the transparency of the nuclei is supposed to increase. It is found from these calculations that the distances of the closest approach are inversely proportional to the energies.

One can, therefore, conclude that it is possible to give a satisfactory account of the elastic scattering of heavy ions at relatively low energies within the Glauber model by releasing the straight-line condition. The usual Glauber formula applies, but the overlap integral must be correctly evaluated taking into account the distortion of the trajectory due to both the strong Coulomb field and the nuclear field. The success of this model is due to the fact that one

has been able to evaluate the overlap integral over the actual heavy-ions trajectories. Thus, it may be concluded that the modified Glauber models I and II have been extended to study the heavy-ion elastic scattering at low energies and have improved the results of the calculations of the elastic scattering and the reaction cross-sections.

References

1. R.M. Devris, J.C. Peng, Phys. Rev. C **22**, 1055 (1980).
2. S.K. Gupta, S. Kailas, Z. Phys. A **317**, 75 (1984).
3. W.Q. Shen, B. Wang, J. Feng, W.L. Zhan, Y.T. Zhu, E.P. Feng, Nucl. Phys. A **491**, 130 (1989).
4. R.E. Warner, G.N. Felder, Phys. Rev. C **42**, 2252 (1990).
5. M.S. Husseinn, R.A. Rego, C.A. Bertulani, Phys. Rep. **201**, 279 (1991).
6. M.E. Brandan, J. Phys. G **9**, 1404 (1983).
7. M. Buenerd, A. Lounis, J. Chauvin, D. Lebrun, P. Martin, G. Duhamel, J.C. Gondrand, P. de Saintgnon, Nucl. Phys. A **424**, 313 (1984).
8. A.J. Cole, W.D. Rae, M.E. Branden, A. Dacal, B.G. Harvey, R. Legrain, M.J. Murphy, R.G. Stoksted, Phys. Rev. Lett. **47**, 1705 (1981).
9. S. Kox, A. Gamp, R. Cherkaoui, A.J. Cole, N. Longequeue, J. Menet, C. Perrin, J.B. Viano, Nucl. Phys. A **420**, 162 (1984).
10. S. Kox, A. Gamp, C. Perrin, J. Arvieux, R. Bertholt, J.F. Bruandet, M. Buenerd, R. Cherkaoui, A.J. Cole, Y. El-Marsi, N. Longequeue, J. Menet, F. Merchez, J.B. Viano, Phys. Rev. C **35**, 1678 (1987) and references therein.
11. Y.G. Ma, W.Q. Shen, J. Feng, Y.Q. Ma, Phys. Rev. C **48**, 850 (1993).
12. R.A. Rego, Nucl. Phys. A **581**, 119 (1995).
13. R.J. Glauber, *Lectures on Theoretical Physics* (Interscience, New York 1959) Vol. **I**.
14. A. Vitturi, F. Zardi, Phys. Rev. C **36**, 1404 (1987).
15. S.M. Lenz, A. Vitturi, F. Zardi, Phys. Rev. C **40**, 2114 (1989).
16. S.M. Lenzi, A. Vitturi, F. Zardi, Phys. Rev. C **38**, 2086 (1988).
17. J. Chauvin, D. Lebrun, A. Lounis, M. Buenerd, Phys. Rev. C **28**, 1970 (1983).
18. S.K. Charagi, S.K. Gupta, Phy. Rev. C **46**, 1982 (1992).
19. A.Y. Abul-Magd, M.T. Al hinai, Nuovo Cimento A **110**, 1281 (1997).
20. C. Xiangzhou, F. Jun, S. Wenqing, M. Yugang, W. Jiansong, Y. Wei, Phys. Rev. C **58**, 572 (1998).
21. S.K. Charagi, Phys. Rev. C **51**, 3521 (1995).
22. M.H. Cha, Phys. Rev. C **46**, 1026 (1992).
23. S.K. Charagi, Phys. Rev. C **48**, 452 (1993).
24. P.J. Karol, Phys. Rev.. C **11**, 1203 (1975).
25. P.J. Karol, Phys. Rev. C **46**, 1988 (1992).
26. S.K. Charagi, S.K. Gupta, Phys. Rev. C **41**, 1610 (1990).
27. S.K. Charagi, et al., Phys. Rev. C **48**, 1152 (1993).
28. J.Y. Hostachy, M. Buenerd, J. Chauvin, D. Lebrun, Ph. Martin, J.C. Lugol, L. Papineau, P. Roussel, N. Alumanos, J. Arvieux, C. Cerruti, Nucl. Phys. A **490**, 441 (1988).
29. S.K. Gupta, P. Shukla, Phys. Rev. C **52**, 3212 (1995).
30. W.Q. Shen, B. Wang, W.-L. Zhan, Y.-t.Zhu, E.P. Feng, Nucl. Phys. A **491**, 130 (1989).
31. H.G. Bohlen et al., Z. Phys. A **308**, 121 (1982).